

Few-Nucleon Calculations and Correlations. *

W. GLÖCKLE, H. KAMADA, J. GOLAK, A. NOGGA

Institut für Theoretische Physik II, Ruhr-Universität Bochum, D44780 Bochum,
Germany

AND

H. WITAŁA, R. SKIBIŃSKI, J. KUROŚ-ŻOŁNIERCZUK

Institute of Physics, Jagellonian University, PL-30059 Cracow, Poland

Present day results for few-nucleon bound state and scattering observables based on modern high precision nuclear forces are briefly reviewed. While in relation to NN forces of that type three-nucleon (3N) forces are mandatory for binding energies and for quite a few 3N scattering observables their effect is rather small in two-nucleon correlation functions as demonstrated for ${}^3\text{He}$ and ${}^4\text{He}$.

The old idea of the Coulomb sum rule as a way to extract the pp correlation function is reconsidered and the need for more accurate data is pointed out. It appears to be an ideal case to probe properties of the density operator and the ground state wave functions without disturbances of final state interactions (FSI).

In the 3N system below the pion threshold FSI is well under control and therefore the exclusive process ${}^3\text{He}(e, e'NN)$ is also a very good test case for correlated nuclear wave functions and electromagnetic current operators. One specific kinematics is emphasized, which can lead to insights into the correlated ground state wave functions with little disturbance of FSI. Finally exclusive photodisintegration of ${}^3\text{He}$ is regarded, which appears to be promising to identify 3N force effects.

PACS numbers: 21.45+v, 21.10-k, 25.10+s, 25.20-x, 27.10+h

1. Introduction

The first and simplest description of nuclear physics is based on the non-relativistic Schrödinger equation. On this stage one requires that NN

* Presented at 5th workshop on "e.-m. induced two-hadron emission"; Lund, Sweden, June 13-16, 2001.

interactions are well tuned to NN data up to the pion threshold and are accompanied by 3N forces, which at least guarantee the correct ${}^3\text{H}$ binding energy. For electromagnetic probes current operators consistent with the nuclear interactions are needed. To get insight into the dynamics of the nuclear systems, reliable solutions of such a Schrödinger equation are necessary. But extensions to this picture are possible. A more advanced and possibly necessary dynamical picture would include relativity for instance in the instant form of a Hamiltonian formalism[1]. Here we restrict ourselves to a strictly nonrelativistic treatment. We employ the present day perfectly well tuned NN forces CD-Bonn[2], AV18[3], Nijmegen I and II[4]. They are mostly of phenomenological and local nature, with the exception of CD-Bonn, which is a slightly modified one-boson-exchange potential and highly nonlocal. As 3N forces we choose the Tucson-Melbourne (TM) 2π -exchange [5] and the Urbana IX [6] models. In the first case the off-shell $\pi - N$ amplitude is used in a low momentum expansion, in the second case that amplitude is based on an intermediate Δ -excitation and a phenomenological short range part. Two strengths parameters in the Urbana IX 3N force are adjusted to the ${}^3\text{H}$ binding energy and nuclear matter density. In the TM 3N force we adjust the cut-off parameter Λ for a strong form-factor parametrization separately for each NN force partner to the ${}^3\text{H}$ binding energy[7]. The 3N system is solved rigorously in the Faddeev scheme for bound and scattering states; the 4N bound state is equally precisely evaluated using Yakubovsky equations[7]. A survey of typical and current results for binding energies and scattering observables is presented in Section II.

Wave function properties in form of bound state two-body correlation functions are shown in Section III. One approach of connecting them to observables is the Coulomb sum rule. We briefly review that topic in Section IV and point to necessary improvements in experiment and theory in order to achieve clear and convincing results in the future.

Another approach in investigating correlations are electron induced two-nucleon emissions, which we study in a specific kinematics for the target nucleus ${}^3\text{He}$. It is shown in Section V that FSI appear to be unavoidable (at least below the pion threshold) but can possibly be reduced to an easily accessible and restricted one. This might enable a search for initial state correlations in a rather controlled manner.

Photon induced two-nucleon emission on ${}^3\text{He}$ as well as the pd break-up appear to be very promising to see 3N force effects. This is illustrated in Section VI. Finally we end with a brief outlook.

Potentials	$E(^3\text{H})$	$E(^3\text{He})$	$E(^4\text{He})$
Nijm 93	-7.668	-7.014	-24.53
Nijm I	-7.741	-7.083	-24.98
Nijm II	-7.659	-7.008	-24.56
AV18	-7.628	-6.917	-24.28
CD-Bonn	-8.013	-7.288	-26.26
Exp.	-8.482	-7.718	-28.30

Table 1. ^3H , ^3He and ^4He binding energy predictions for several NN potential models compared to the experimental values. All energies are given in MeV.

2. Three-and Four-Nucleon Systems

A first necessary test of the dynamical picture are three-and four-nucleon binding energies. For five modern, high precision NN forces our theoretical results are shown in Table 1. We have taken into account charge independence and charge symmetry breaking as well as the mass difference of the proton and the neutron. Further electromagnetic interactions are included and also the isospin $T = \frac{3}{2}$ admixtures. We see the by now well known under binding against the experimental values. Table 2 collects the individually adjusted Λ -parameters of the TM 3N force and of a modified one (TM'), which violates chiral invariance less than TM, and the resulting 3N and 4N binding energies. We also show the AV18 plus Urbana IX results. We end up with the interesting result that the theoretical α -particle binding energies for the different NN and 3N force combinations are rather close to the experimental value. There is a slight over binding, which leaves little room for the action of 4N forces. This can be quantified in the following way. The average attraction due to NN forces is 24.92 MeV or 88 % from 28.30 MeV. The average additional attraction due to 3N forces is 3.9 MeV or 14 % and finally the average over binding is 0.5 MeV, which is 2 % of 28.30 MeV. If as a conjecture this would be attributed to a repulsive 4NF then this shows a nice hierarchy in the importance of two- to many-body forces. Of course this is a temporary statement and can be modified in the future if more will be known about strengths and properties of 3N forces. In any case such a hierarchy is in agreement with the expectations of chiral perturbation theory[9, 10]. An overview of 3N and 4N binding energies is shown in Fig. 1, which documents the strong correlation among them, known as Tjon line [7, 8].

The Argonne-Illinois-Los Alamos collaboration has explored with the

Potentials	$\Lambda [m_\pi]$	$E(^3\text{H})$	$E(^3\text{He})$	$E(^4\text{He})$
CD-Bonn+TM	4.784	-8.478	-7.735	-29.15
AV18+TM	5.156	-8.478	-7.733	-28.84
AV18+TM'	4.756	-8.448	-7.706	-28.36
AV18+Urbana IX	—	-8.484	-7.739	-28.50
Exp.	—	-8.482	-7.718	-28.30

Table 2. ^3H , ^3He and ^4He binding energy predictions for several NN and 3N potential models compared to the experimental values. All energies are given in MeV.

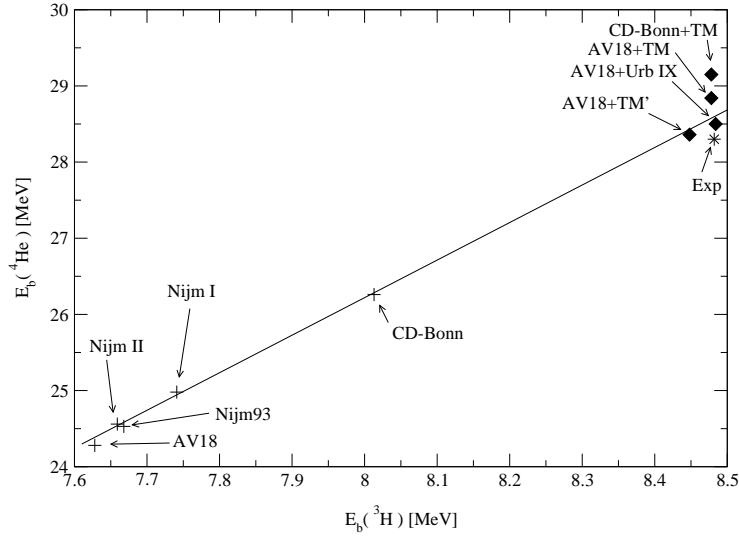


Fig. 1. Tjon-line: α -particle binding energy predictions $E(^4\text{He})$ against the predictions for the ^3H binding energy for several interaction models. Predictions without (crosses) and with (diamonds) 3N forces are shown. The experimental point is marked by a star. The line represents a least square fit to NN force predictions only.

help of the Greens-Function Monte Carlo method the low energy spectra of light nuclei up to $A=8$ [11]. We see in Fig. 2 the pure AV18 predictions,

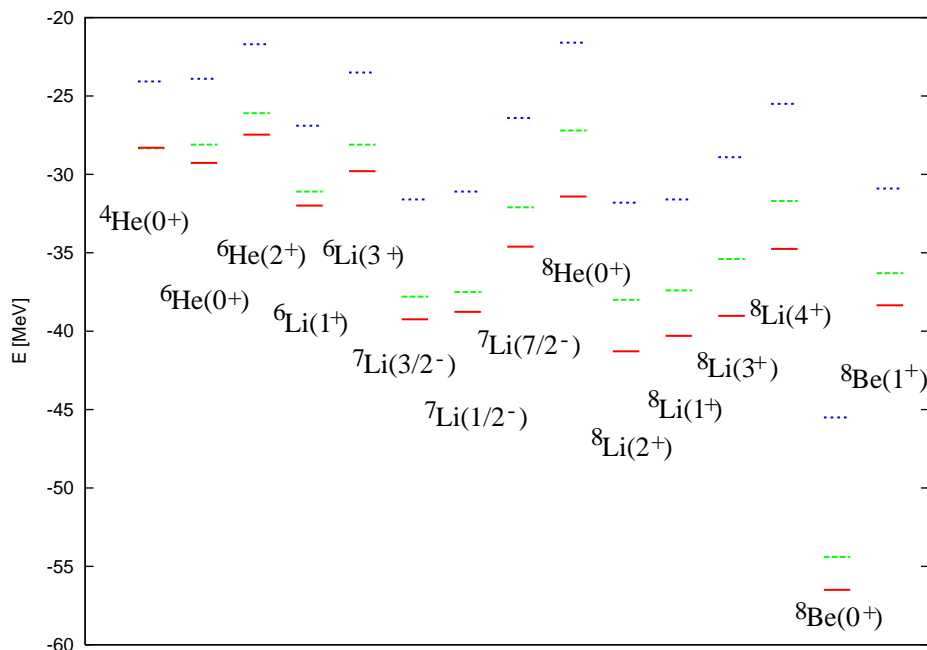


Fig. 2. Spectra of light nuclei: experimental data (red,solid), AV18 (blue,dotted), AV18+Urbana IX (green,dashed).

which are rather far away from the data and the impressive shift of theory towards the data by adding the Urbana IX 3N force. But we still observe deviations, which can be resolved by including additional terms in the 3NF [12]. Further important tests of the nuclear Hamiltonian without and with 3N forces are scattering processes. For three nucleons solutions for the continuum are by far most developed. The Faddeev scheme [13] and the hyperspherical harmonic method [14] provide very accurate solutions. We illustrate the state of art with several cross sections and refer the reader to [13] and more recent papers [15, 16, 17] for a larger overview and for the very many spin observables, which probe our present day understanding of the dynamics in a very sensitive manner. Fig. 3 shows the nd total cross section, which below about 100 MeV is nearly perfectly described even without 3N forces. Only at the higher energies small discrepancies appear, which are however significantly reduced including 3N forces. At very low energies the inclusion of the pp Coulomb force is under control. For a survey on the beautiful agreement of the angular distribution in elastic

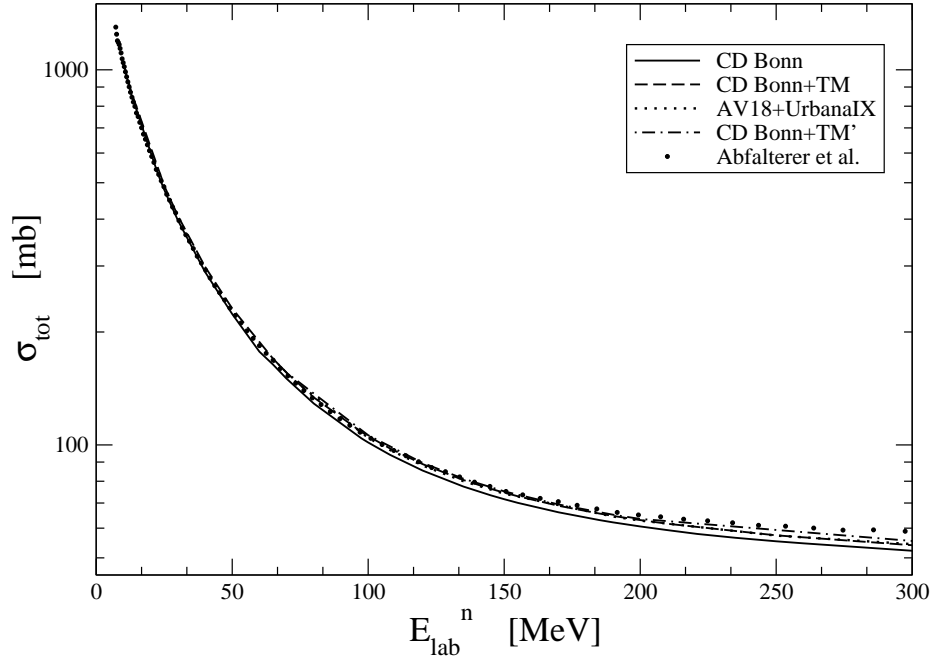


Fig. 3. The total nd cross section. Comparison of the data [33] with various interaction models.

pd scattering with precise data we refer to [14]. Thereby 3N force effects are tiny. This remains true also at somewhat higher energies as shown in Fig. 4, where the theory does not include the Coulomb forces nor 3N forces. At 65 and 135 MeV theory based on NN forces only clearly underestimates the data in the minima whereas the inclusion of 3N forces leads to a very good agreement. This is shown in Figs. 5 and 6. Thereby the results, as shown by two bands, are very stable under exchange of NN and 3N force combinations (which of course describe the ${}^3\text{H}$ binding energy). Finally we show in Figs. 7 and 8 some break-up cross sections along the kinematical locus as a function of a suitably defined arclength S [13]. In general the agreement is good and at those low energies 3N force effects studied up to now are insignificant.

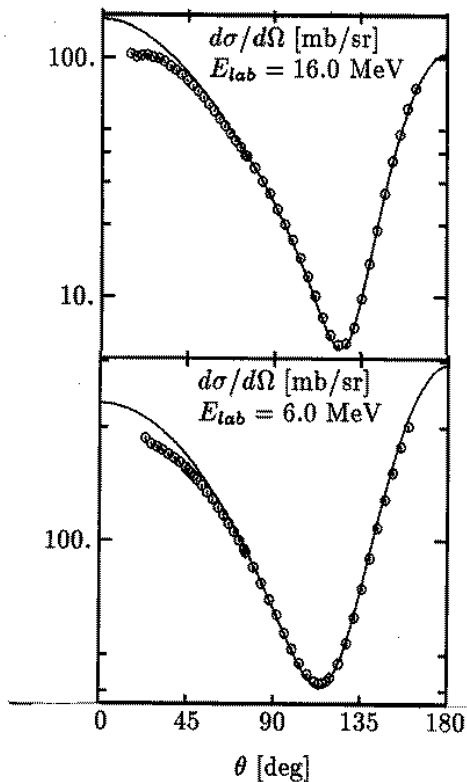


Fig. 4. Differential cross section for elastic nucleon-deuteron scattering. pd data from [18].

A prerequisite to a theoretical analysis of ${}^3\text{He}(e, e'\text{NN})$ data is the understanding of the $d(p, \text{NN})$ reaction in the full phase space. Therefore 4π -measurements of the latter process, not only at certain selected regions in phase space, are quite important to test the theory, before conclusions can be drawn from an analysis of the ${}^3\text{He}(e, e'\text{NN})$ reaction.

However, overall one can already say now that the dynamical picture with high precision NN forces and adjusted 3N forces works reasonably well (with room for improvements) and provides a good basis to analyze electromagnetically induced processes.

3. Two-Nucleon Correlation Functions

Based on fully converged solutions of the Faddeev-Yakubovsky equations we present two-nucleon correlation functions for ground state wave functions $|\Psi JM\rangle$ of the simplest type, namely averaged over two-body partial wave states:

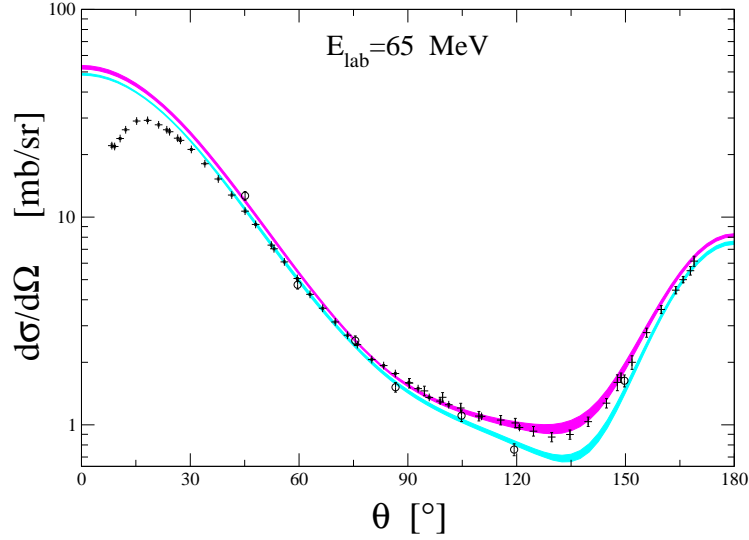


Fig. 5. Differential cross section in elastic Nd scattering at 65 MeV. The light (dark) shaded bands are NN force only (NN+3NF) predictions for various interactions. pd data (crosses) are from [19] and nd data (open circles) are from [20].

$$C(r) = \frac{1}{2J+1} \sum_M \langle \Psi JM | \delta(\vec{r} - \vec{r}_{ij}) P_{ij} | \Psi JM \rangle \quad (1)$$

Here \vec{r}_{ij} is the operator of a pair distance and P_{ij} the projector on a pp or np pair. They are plotted (with arbitrary overall normalization) in Fig. 9 for d , ${}^3\text{He}$ and ${}^4\text{He}$ and choosing two NN potentials AV18 and CD Bonn. At short distances below about 1 fm the predictions of the two potential are quite different. The curves are very much similar for the three nuclei, what suggests that this will essentially remain true also for heavier systems. They all peak at about 1 fm. Fig. 10 compares directly predictions for the three nuclei, all normalized to each other in the peak value. We see a nearly perfect overlap except in the tails, where the difference in separation energies show up. Finally the addition of 3N forces has no visible influence up to the radii somewhat larger than 1 fm, where binding effects have to appear.

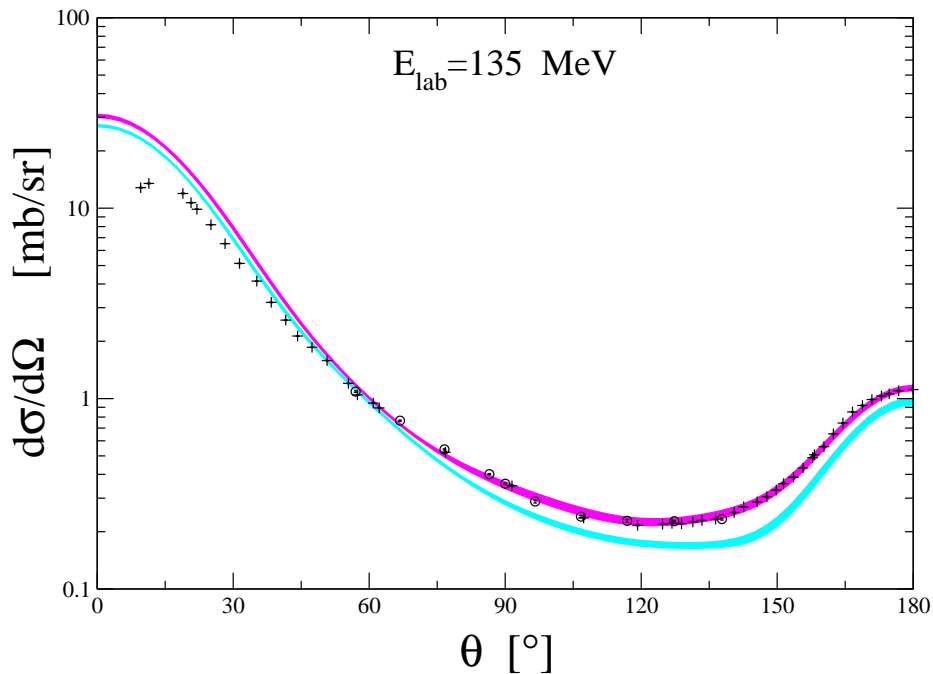


Fig. 6. The same as in Fig. 5 for $E = 135$ MeV. pd data (crosses) are from [21] and (circles) from [22].

Since wave functions are not observables, in consequence the wave function property $C(r)$ is not an observable either. Wave functions enter into observable response functions as they occur for instance in electromagnetically induced processes, but they are accompanied by final state continuum wave functions, which are also correlated and, very importantly, they come together with current operators, which should be consistent to the nuclear forces. Consistent ingredients of the nuclear matrix elements should lead to the same observables (response functions) even if different NN force parameterizations have been chosen. At present mostly AV18 NN forces and consistent currents are being used. Thus work remains to be done to understand possible model dependences.

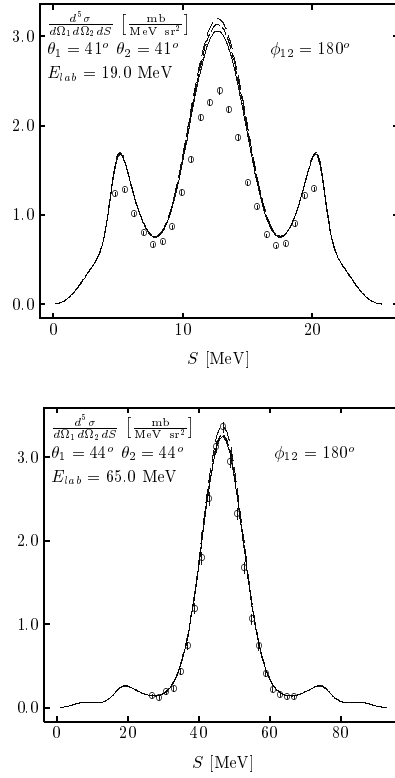


Fig. 7. Five-fold differential Nd breakup cross section along the kinematical locus including the quasi-free scattering condition. pd data at 19 MeV are from ref. [23] and at 65 MeV from ref. [24].

4. The Coulomb Sum Rule

It has been known for a long time [27, 28] that the Coulomb sum rule is an approach to isolate the Fourier transform of the correlation function $C(r)$. Let's define the Coulomb sum as

$$S_L \equiv \int_{\omega_{min}}^{\infty} d\omega R_L(\omega, |\vec{Q}|) \quad (2)$$

Then using the standard expression for the longitudinal response function R_L in inclusive electron scattering together with the closure relation one easily finds [29]

$$S_L = \frac{1}{2} \sum_M \langle \Psi JM | \rho^\dagger \rho | \Psi JM \rangle - \frac{1}{2} \sum_M |\langle \Psi JM | \rho | \Psi JM \rangle|^2 \quad (3)$$

This very nice intermediate result shows that the final state interactions have been totally removed and only ground state expectation values remain.

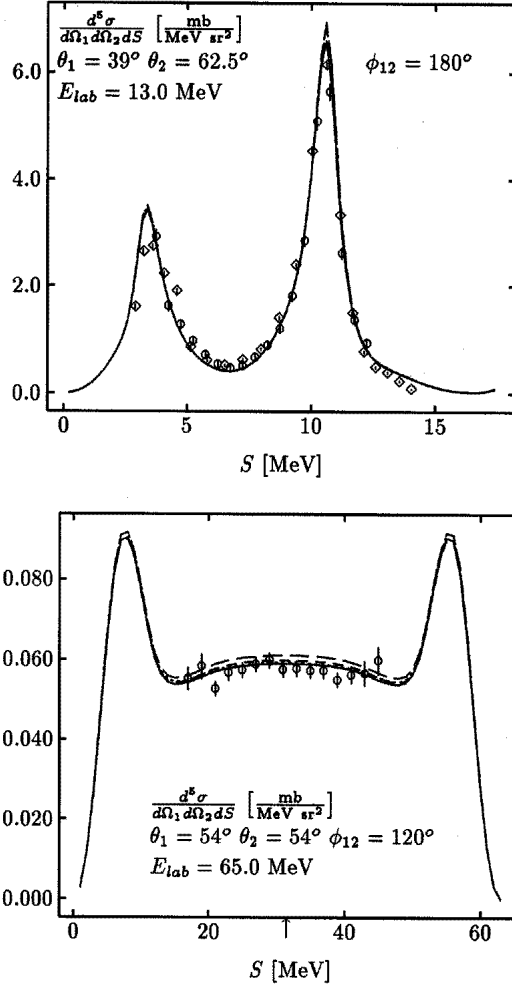


Fig. 8. The same as in Fig. 7 for two cases: two nucleons leave with equal momenta (up) and three nucleons leave with equal energies under pairwise angles of 120° (down). pd data at 13 MeV are from ref. [25], at 65 MeV from ref. [26].

Separating the density operator ρ into single particle and two- and more-particle parts one easily arrives at

$$S_L = ZG_E^p(\vec{Q})^2 + NG_E^n(\vec{Q})^2 - Z^2F_{ch}^2(\vec{Q}) + C(\vec{Q}) + \tilde{C}(\vec{Q}) \quad (4)$$

where $G_E^{p,n}$ are the p, n electric form factors (neglecting the time component

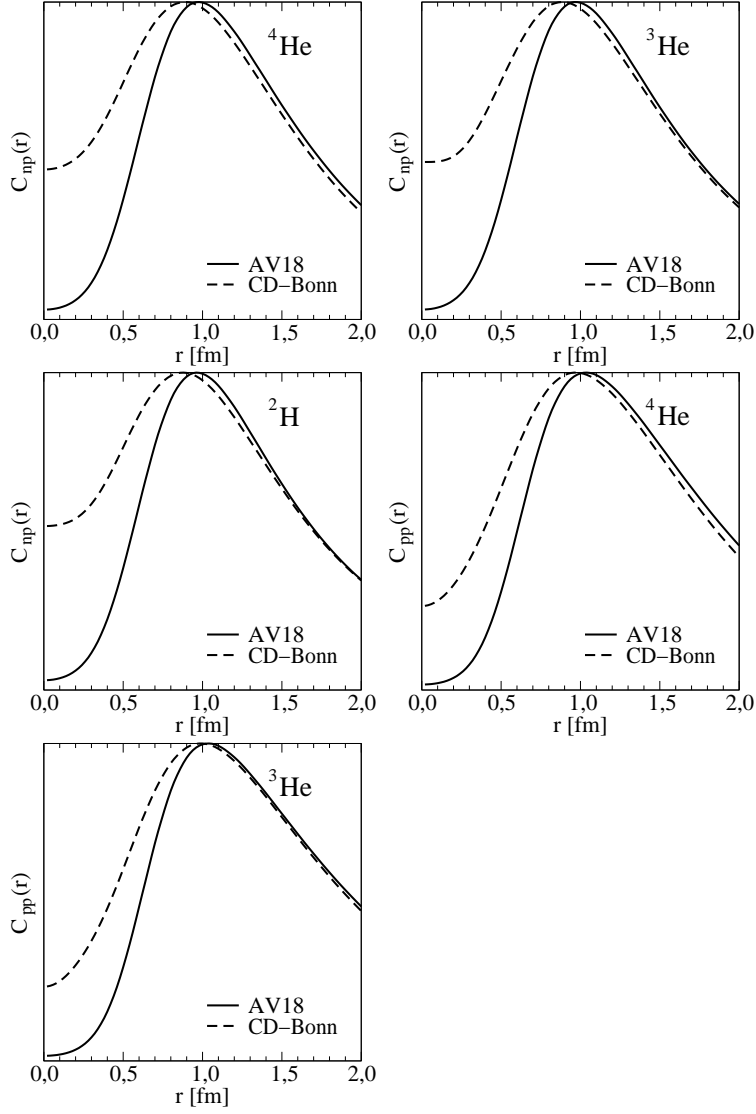


Fig. 9. Two-nucleon correlation functions $C(r)$ for np and pp pairs in the nuclei d , ${}^3\text{He}$ and ${}^4\text{He}$ based on the AV18 and CD Bonn NN potentials.

of the four vector dependence in Q^2), F_{ch} is the elastic charge form factor of the target nucleus, $\tilde{C}(\vec{Q})$ arises from the two- and more-particle densities and

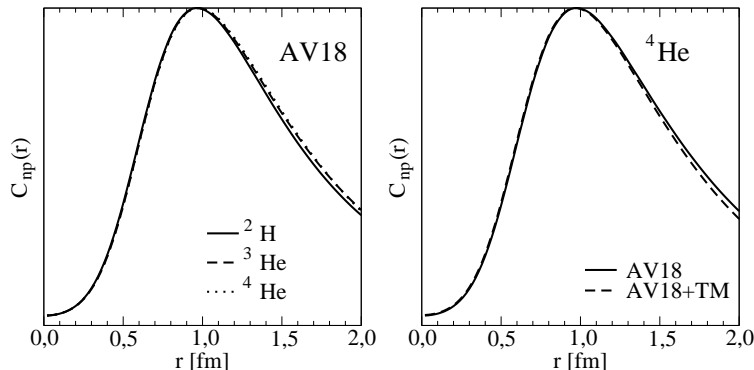


Fig. 10. Comparison of $C(r)$'s for d , ${}^3\text{He}$ and ${}^4\text{He}$ (left) and for AV18 against AV18+TM (right).

$$C(\vec{Q}) \equiv \int d^3r e^{i\vec{Q}\cdot\vec{r}} C(r) \quad (5)$$

is the quantity related to $C(r)$ suitably augmented by the nucleon electromagnetic form factors [29].

There are certain obstacles to be overcome. The integral in Eq. 2 requires an extrapolation to catch all of the integrand above the quasi elastic peak. Up to now the available data leave too much room for ambiguities in the extrapolation [29] and precise data at some more higher ω -values would be welcome. Also the first three terms on the right hand side of Eq. 4 cancel strongly [29] leading to enhanced error bars for C and \tilde{C} . Therefore high accuracy measurements of R_L are needed. Above all this refers to the nuclei ${}^3\text{He}$ and ${}^4\text{He}$, for which at present the most precise evaluation of the ground state wave functions are possible. On the theoretical side as has been shown in [30] the relativistic corrections in the density operator and two-body pieces therein play an important role and cannot be considered as a small perturbation. This is an interesting challenge for theory and experiment and deserves a renewed effort despite the intensive work in the past.

5. Exclusive Electron Scattering on ${}^3\text{He}$

Another approach towards correlations is via electron induced two-nucleon emission on nuclei, here on ${}^3\text{He}$. The most ideal situation would be that one nucleon absorbs the photon and receives its full momentum and all three nucleons leave the nucleus without any final state interaction (FSI). Then the

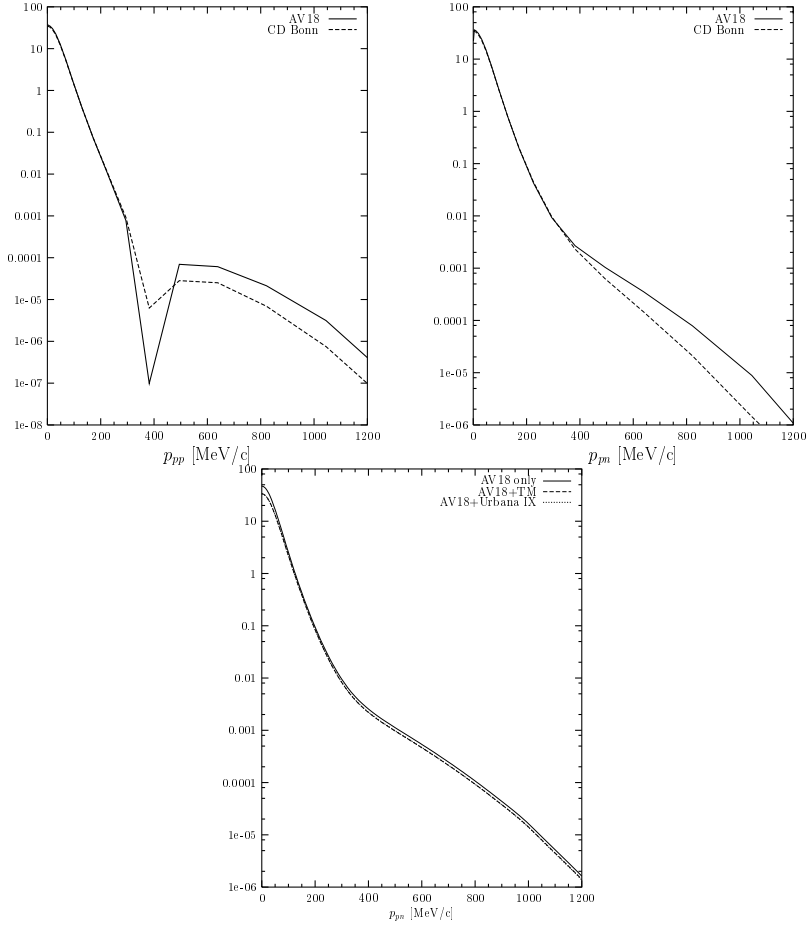


Fig. 11. The expression in Eq. 6 against the relative momentum p for a pp pair (left) and for a np pair (right). Both refer to NN forces only, whereas the figure in the middle includes in addition 3N forces.

measurement of the momenta of the two spectator nucleons would display directly their momentum distribution in ${}^3\text{He}$. For this special kinematics the total spectator pair momentum has to be zero and those two nucleons leave back to back and show directly the relative momentum dependence within a pair of nucleons in the target nucleus ${}^3\text{He}$. Let us number the nucleons such that the knocked out nucleon is number 1. Then one would probe directly the expression related to the ${}^3\text{He}$ wave function

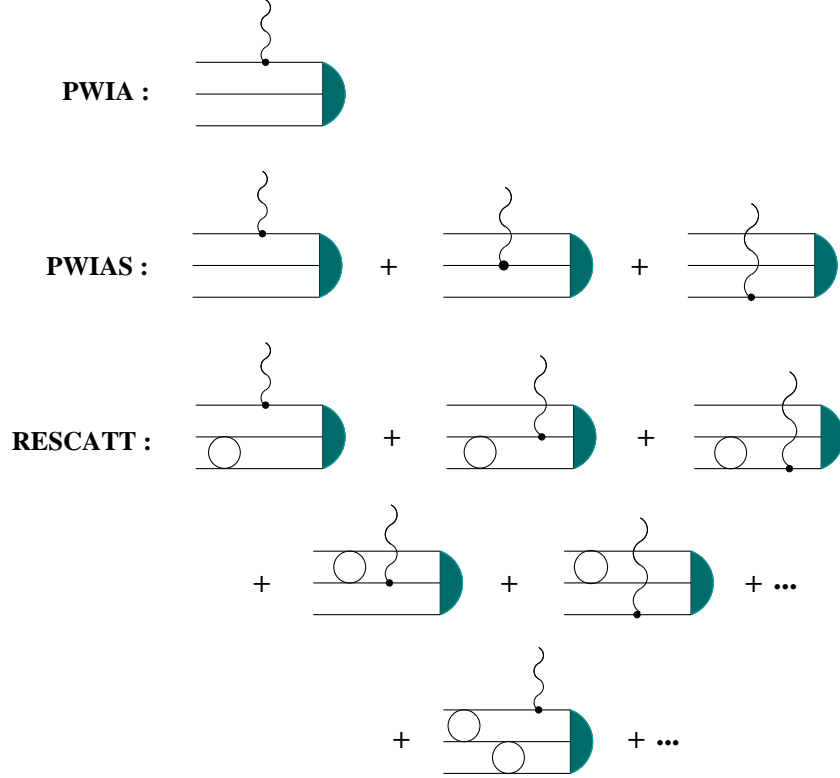


Fig. 12. The matrix elements of Eq. 12 contributing to PWIA, PWIAS and to the infinite number of RESCATT processes. The first diagram in the group RESCATT is the expression “ tG_0 ”.

$$\sum_M \sum_{m_1 m_2 m_3} |\Psi(\vec{p}, \vec{q} = 0)|^2 \quad (6)$$

where $\vec{p} = \frac{1}{2}(\vec{k}_2 - \vec{k}_3)$ and $\vec{q} = \frac{2}{3}(\vec{k}_1 - \frac{1}{2}(\vec{k}_2 + \vec{k}_3))$. The $\vec{k}_i, i = 1, 2, 3$ are the individual momenta. This quantity is plotted in Fig. 11 for the two spectator pairs pp and np and the two NN forces AV18 and CD-Bonn. We see model independence below about $p = 1 \text{ fm}^{-1}$ and significant model dependence at higher p -values. 3N force effects are, like for $C(r)$, quite insignificant as shown in Fig. 11 for a np pair.

Unfortunately reality is far from that ideal situation. FSI interferes very strongly. The eightfold differential cross section has the well known form

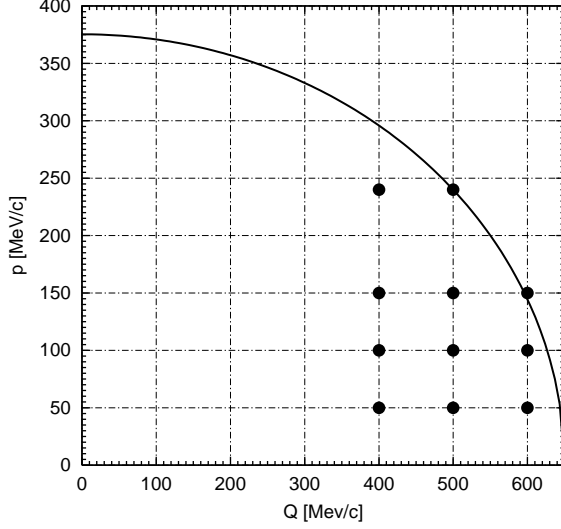


Fig. 13. The restrictions for relative NN momenta p as a function of photon momenta $|\vec{Q}|$ choosing $E_{c.m.}^{3N} = 140$ MeV.

$$\frac{d^8\sigma}{d\hat{k}'dk'_0d\Omega_1d\Omega_2dS} = \sigma_{Mott} (v_L R_L + v_T R_T + v_{TT} R_{TT} + v_{TL} R_{TL}) \rho \quad (7)$$

where the v 's and ρ are kinematical quantities, and the response functions R are

$$\begin{aligned} R_L &= |N_0|^2 \\ R_T &= |N_1|^2 + |N_{-1}|^2 \\ R_{TT} &= 2\text{Re}(N_1 N_{-1}^*) \\ R_{TL} &= -2\text{Re}(N_0(N_1 + N_{-1})^*) \end{aligned} \quad (8)$$

Here enter the nuclear matrix elements N_i , which are the spherical components of

$$N^\mu = 3\langle\Psi^{(-)}|j^\mu(\vec{Q})|\Psi_{3He}\rangle \quad (9)$$

with

$$j^\mu(\vec{Q}) = j^\mu(\vec{Q}, 1) + j^\mu(\vec{Q}, 23) + \dots \quad (10)$$

Note that both 3N states in Eq. 9 are fully antisymmetrized. Using a Faddeev decomposition, N^μ can be written as

$$N^\mu = N_{PWIAS}^\mu + N_{RESCATT}^\mu \quad (11)$$

where

$$\begin{aligned} N_{PWIAS}^\mu &= 3\langle\Phi_{\vec{p}\vec{q}}^0|(1+P)j^\mu(\vec{Q})|\Psi_{3He}\rangle \\ N_{RESCATT}^\mu &= 3\langle\Phi_{\vec{p}\vec{q}}^0|(1+P)|U^\mu\rangle \end{aligned} \quad (12)$$

and $|U^\mu\rangle$ obeys a Faddeev-like integral equation [34]

$$|U^\mu\rangle = tG_0(1+P)j^\mu(\vec{Q})|\Psi_{3He}\rangle + tPG_0|U^\mu\rangle \quad (13)$$

The bra-vectors of Eq. 12 is given by the free momentum eigenstates

$$|\Phi_{\vec{p}\vec{q}}^0\rangle = (1 - P_{23})|\vec{p}\rangle|\vec{q}\rangle \quad (14)$$

antisymmetrized in the pair (23), t is the NN t-operator and G_0 the free 3N propagator. Finally P is the sum of a cyclic and anticyclic permutation of 3 objects. It is instructive to display the physical content of Eq. 12 graphically in Fig. 12. There the different treatments of the final state, PWIA, PWIAS, “ tG_0 ” and “full” are explained. It is easy to show that in PWIA one finds

$$\begin{aligned} R_L &= G_E^2(\vec{Q})\frac{1}{2}\sum|\Psi(\vec{p},\vec{q}=0)|^2 \\ R_T &= \frac{\vec{Q}^2}{2m_N^2}G_M^2(\vec{Q})\frac{1}{2}\sum|\Psi(\vec{p},\vec{q}=0)|^2 \end{aligned} \quad (15)$$

and $R_{TT} = R_{TL} = 0$. Thus R_L and R_T provide access to the same quantity $\sum|\Psi|^2$ up to known factors. The most simple approximate FSI is the action of t within the spectator pair of nucleons, called “ tG_0 ” below in Figs. 14–17 Since we are restricting ourselves to a nonrelativistic framework the total 3N c.m. energy should be below the pion threshold at 140 MeV. Then for given $|\vec{Q}|$ the p-values are restricted as shown in Fig. 13. For three $|\vec{Q}|$ -values, 400, 500, 600 MeV/c, we compare in Fig. 14 the quantity $R_L/(F_1^p)^2$ for PWIA, PWIAS, “ tG_0 ”, and using the complete FSI (called Full), as a function of the relative momentum of an outgoing np pair. In PWIA \vec{p} is related to the spectator pair (the above mentioned pair 23). Consequently it is assumed that the knocked-out nucleon is a proton. Of course for PWIA there is no $|\vec{Q}|$ -dependence and we see directly the expression given in Eq. 6. FSI has a tremendous effect for all three $|\vec{Q}|$ -values, however the simple approximation “ tG_0 ” improves going to the higher $|\vec{Q}|$ -values. Even for higher $|\vec{Q}|$ values FSI has a tremendous effect on R_L (a reduction factor 10-100). At least for the higher $|\vec{Q}|$ values the tG_0 approximation might be reasonable, but still one can see effects of the neglected FSI of spectator nucleons and hit proton. In case of R_T we show in Fig. 14 the ratio $(2m_N^2 R_T)/(G_M^p Q)^2$. In addition some curves include π and ρ exchange contributions consistent to AV18.

Their effect is totally negligible. Also in this case the approximation “ tG_0 ” is a quite good representation of the full FSI. Since that FSI correction of first order in t is very well under control given the fact that the on-shell t is fitted to the NN data, an analysis of future data appears to be a rather reliable approach towards the quantity given in Eq. 6. There is nice stability under exchange of the NN forces AV18 against CD Bonn, as shown in Fig. 15 for the example $|\vec{Q}|=400$ MeV/c.

The situation is quite different if the hit nucleon is a neutron. We show in Fig. 16 the quantity $R_L/(G_E^n)^2$. In contrast to the case before, the approximate FSI treatment “ tG_0 ” is now totally different from the complete FSI result and thus would be totally misleading. This is of course due to the smallness of G_E^n . For R_T , however, the “ tG_0 ” approximation and “Full” are not far from each other and moreover the $|\vec{Q}|$ -dependence is relatively weak. Nevertheless for both R 's the predictions are nearly independent from the specific choice of the NN force as shown in Fig. 17 and therefore the model dependence is weak.

All the curves in Figs. 14 and 16 refer to AV18 and the angle between \vec{p} and \vec{Q} has arbitrarily been fixed at 90° . At the other angles the relation between the “full” result and the “ tG_0 ” approximation changes, but remains within the same order of magnitude.

Based on these results one has to state that there is no way to access directly in that low energy regime $\sum |\Psi|^2$. Nevertheless precise measurements would be extremely informative to test the whole dynamical picture, forces and currents. Choosing other kinematical conditions even in PWIA the ${}^3\text{He}$ bound state $\Psi(\vec{p}, \vec{q})$ is probed in such a manner that both \vec{p} and \vec{q} vary. Under the prerequisite that the pd break-up process has been tested carefully against theory the ${}^3\text{He}(e, e'NN)$ reaction for general kinematics is a perfect tool to probe the remaining unknown ingredient, the current operator [31].

6. 3N Force Effects in Photo-Induced Disintegration of ${}^3\text{He}$

3N forces are required for a correct description of binding energies. Will they also play a role in electromagnetically induced processes? We already started a first investigation for pd capture processes in [32] and would like to show new results for photodisintegration of ${}^3\text{He}$, specifically at higher energies than the one considered in [32]. To that aim the Faddeev-like integral equation in [34] has to be modified. The nuclear matrix element for ${}^3\text{He}(\gamma, NN)$

$$N^\mu = \langle \Psi_{\vec{p}\vec{q}}^{(-)} | j^\mu | \Psi_{3He} \rangle \quad (16)$$

can be written as

$$N^\mu = \frac{1}{2} \langle \Phi_{\vec{p}\vec{q}}^0 | (1 + tG_0) P | \tilde{U}^\mu \rangle \quad (17)$$

where $|\tilde{U}^\mu\rangle$ obeys the Faddeev-like integral equation

$$|\tilde{U}^\mu\rangle = (1 + P) j^\mu |\Psi_{^3\text{He}}\rangle + (tG_0 P + \frac{1}{2}(1 + P) V_4^{(1)} G_0 (1 + tG_0) P) |\tilde{U}^\mu\rangle \quad (18)$$

We use the Siegert theorem as described in [32]. This includes some of the exchange currents. The operator $V_4^{(1)}$ is that part of the 3N force, which is symmetric under the exchange of particle 2 and 3. We scanned the whole phase space comparing the full break-up cross section evaluated with and without 3N force. As an example we display in Fig. 18 the θ_1, θ_2 regions where 3N force effects are larger than 40 %. The relative azimuthal angle is $\leq 50^\circ$.

As an illustration we show out of that phase space region three more or less arbitrarily selected break-up cross sections along the S -curve in Figs. 19–20. The peak in the middle is caused by small relative momenta in one pair (FSI peak). In the other peaks the ^3He wave function is probed at small momenta. Measurements should validate or invalidate these sort of predictions. Also in the pd break-up process 3NF effects are clearly visible as shown in Fig. 21 for various photon energies.

7. Outlook

One main theoretical challenge is to establish an electromagnetic current operator, which is consistent to nuclear forces. Only then response functions for electromagnetically induced processes can be put on a firm ground. Precise experimental data on two-nucleon emissions induced by real and virtual photons on ^3He will be a very important test ground to probe nuclear forces, correlated wave functions and currents. At present the 3N system is the only case where FSI is fully under control (below the pion threshold) and appears therefore especially promising to probe our present day understanding of nuclear dynamics.

Acknowledgments

This work has been supported by the DFG (J.G.) and the Polish Committee for Scientific Research under Grant No. 2P03B02818. The numerical calculations have been performed on the Cray T90 and T3E of the NIC in Jülich, Germany.

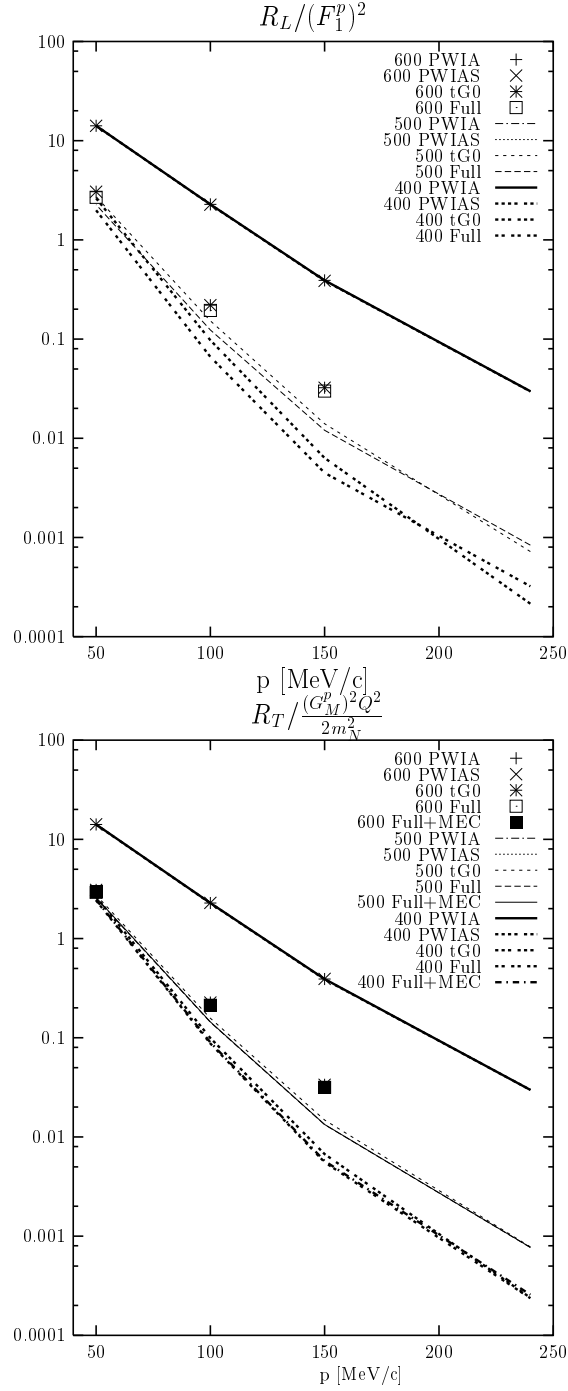


Fig. 14. $R_L/(F_1^p)^2$ (up) and $(2m_N^2 R_T)/(G_M^p Q)^2$ (down) against the np relative momentum p for various treatments of the final 3N state and the $|\vec{Q}|$ -values 400, 500 and 600 MeV/c. MEC effects are negligible as shown.

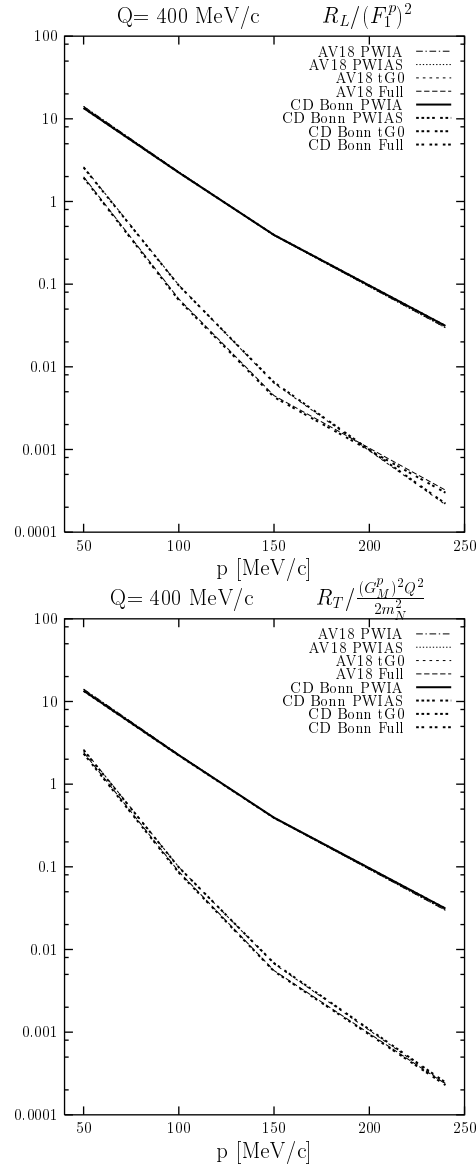


Fig. 15. $R_L/(F_1^p)^2$ (up) and $(2m_N^2 R_T)/(G_M^p Q)^2$ (down) against the np relative momentum p for various treatments of the final $3N$ state and two different potentials at one $|\vec{Q}|$ -value.

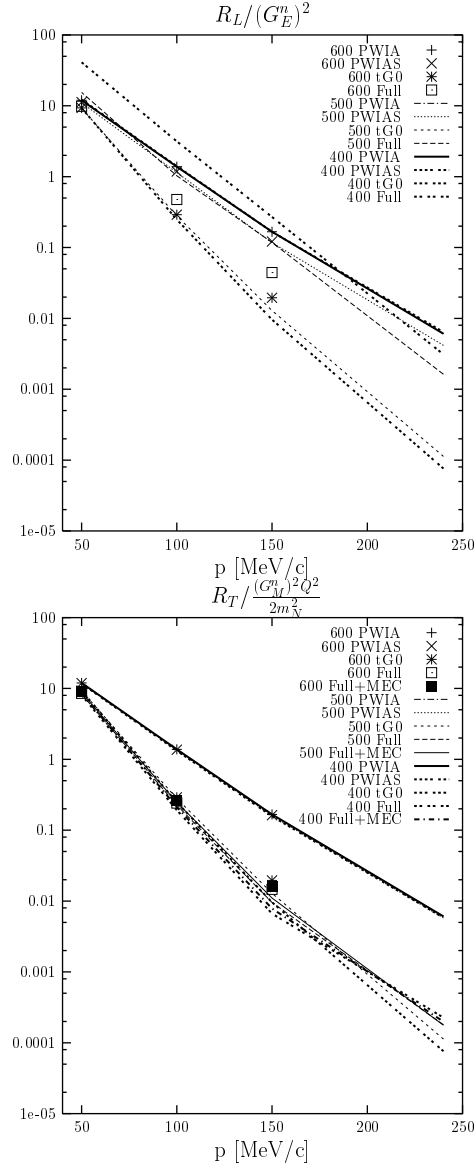


Fig. 16. $R_L / (G_E^n)^2$ (up) and $(2m_N^2 R_T) / (G_M^n Q)^2$ (down) against the pp relative momentum p for various treatments of the final 3N state and some $|\vec{Q}|$ -values. MEC effects are negligible as shown.

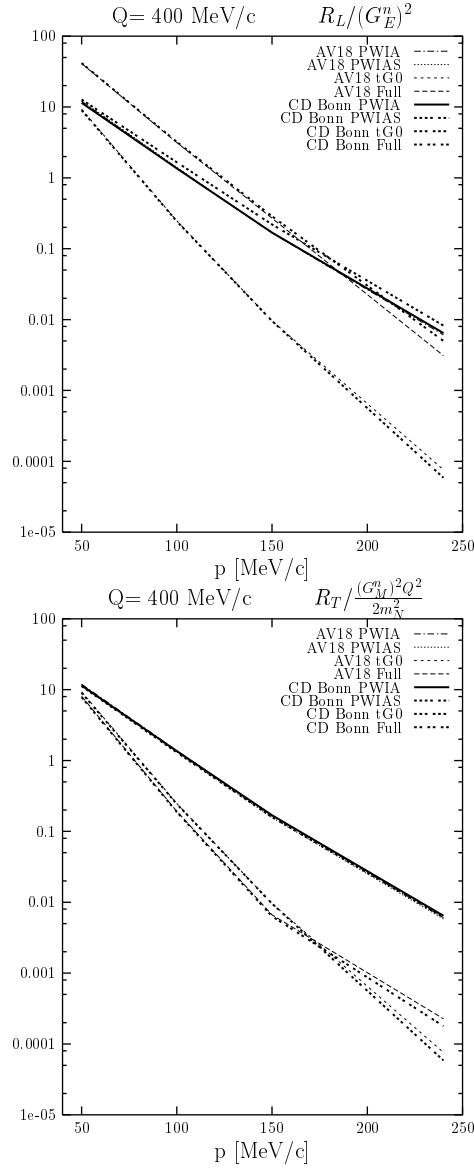


Fig. 17. $R_L/(G_E^n)^2$ (up) and $(2m_N^2 R_T)/(G_M^n Q)^2$ (down) against the pp relative momentum p for various treatments of the final $3N$ state and two different potentials at one $|\vec{Q}|$ -value.

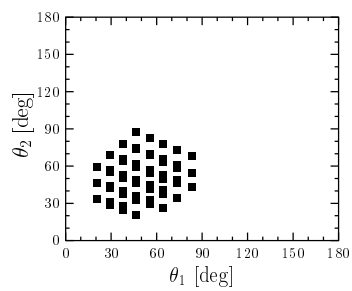


Fig. 18. The θ_1 - θ_2 regions in 3N phase space, where 3N force effects are larger than 40 %. The relative azimuthal angle is $\phi_{12} \leq 50^\circ$.

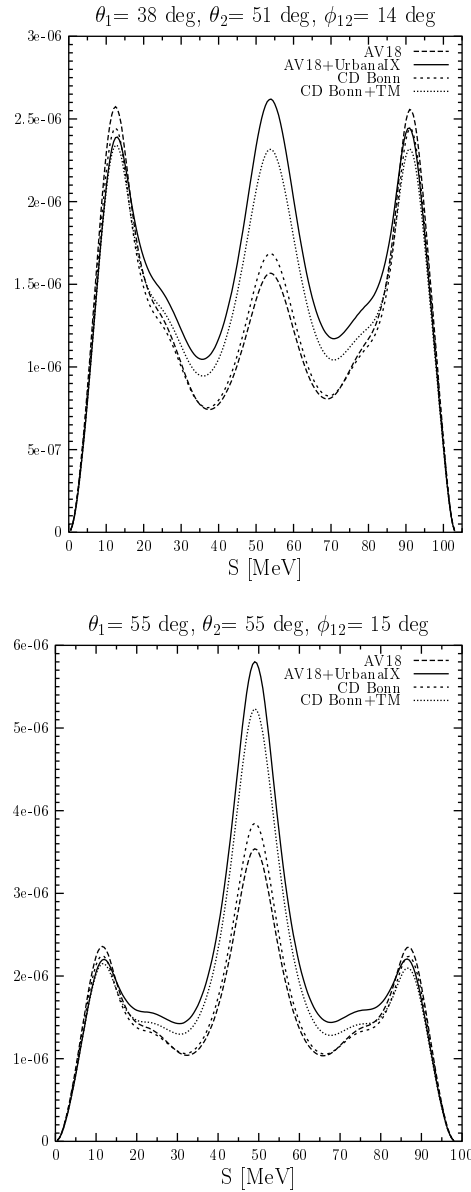


Fig. 19. Three-body differential photodisintegration cross sections $d^3\sigma/(d\Omega_1 d\Omega_2 dS)$ [$\text{fm}^2/(\text{sr}^2\text{MeV})$] of ^3He along the kinematical locus for different combinations of angles.

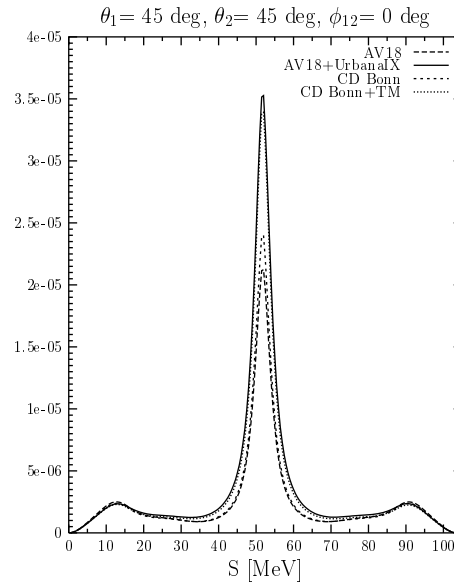


Fig. 20. The same as in Fig. 19 for a specific breakup configuration, where two nucleons leave with equal momenta leading to a FSI peak.

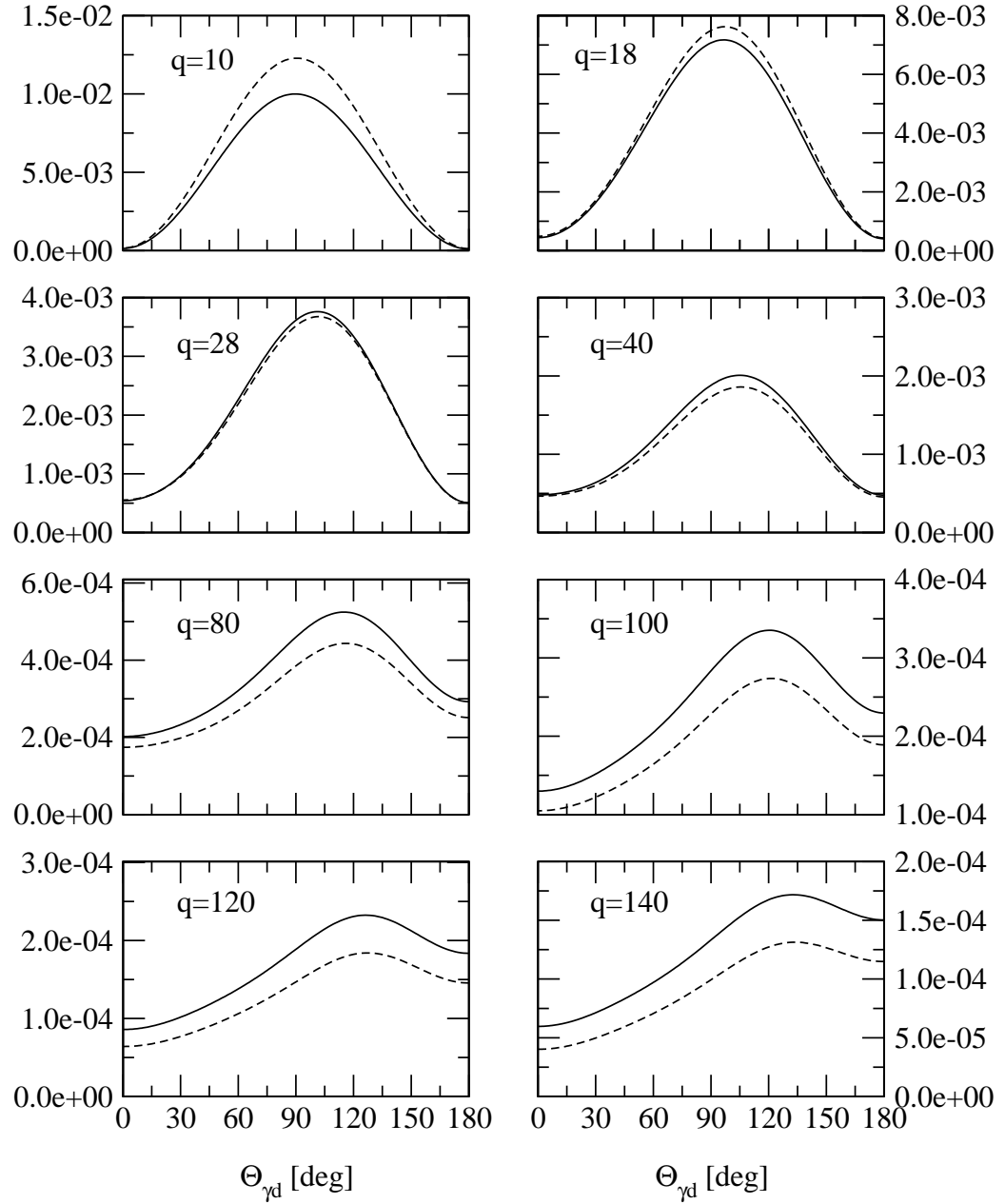


Fig. 21. The pd photodisintegration breakup cross section $d\sigma/d\Omega_d$ [fm²/sr] of ^3He based on AV18 alone (dashed curve) and AV18+Urbana IX (solid curve) for various photon energies q in MeV.

REFERENCES

- [1] W. Glöckle, T.-S. H. Lee, F. Coester, *Phys. Rev. C* **33**, 709 (1986).
- [2] R. Machleidt, *Phys. Rev. C* **63**, 024001 (2001).
- [3] R. B. Wiringa, V. G. J. Stoks, R. Schiavilla, *Phys. Rev. C* **51**, 38 (1995).
- [4] V. G. J. Stoks, R. A. M. Klomp, C. P. F. Terheggen, J. J. de Swart, *Phys. Rev. C* **49**, 2950 (1994).
- [5] S. A. Coon *et al.*, *Nucl. Phys. A* **317**, 242 (1979).
- [6] B. S. Pudliner *et al.*, *Phys. Rev. C* **56**, 1720 (1997).
- [7] A. Nogga, H. Kamada, W. Glöckle, *Phys. Rev. Lett.* **85**, 944 (2000).
- [8] J. A. Tjon, *Phys. Lett. B* **56**, 217 (1975).
- [9] U. van Kolck, *Phys. Rev. C* **49**, 2932 (1994).
- [10] C. Ordóñez *et al.*, *Phys. Rev. C* **53**, 2086 (1996).
- [11] R. B. Wiringa *et al.*, *Phys. Rev. C* **62**, 014001 (2000).
- [12] Steven C. Pieper *et al.*, *Phys. Rev. C* **64**, 014001 (2001).
- [13] W. Glöckle, H. Witała, D. Hüber, H. Kamada and J. Golak, *Phys. Rep.* **274**, 107 (1996).
- [14] A. Kievsky *et al.*, *Nucl. Phys. A* **607**, 402 (1996); *Phys. Rev. C* **64**, 024002 (2001).
- [15] H. Witała *et al.*, *Phys. Rev. C* **63**, 024007 (2001).
- [16] R. V. Cadman *et al.*, *Phys. Rev. Lett.* **86**, 967 (2001).
- [17] W. Glöckle *et al.*, *Nucl. Phys. A* **684**, 184c (2001).
- [18] K. Sagara *et al.*, *Phys. Rev. C* **50**, 576 (1994).
- [19] H. Shimizu *et al.*, *Nucl. Phys. A* **382**, 242 (1982).
- [20] H. Rühl *et al.*, *Nucl. Phys. A* **524**, 377 (1991).
- [21] H. Sakai *et al.*, *Phys. Rev. Lett.* **84**, 5288 (2000).
- [22] N. Sakamoto *et al.*, *Phys. Lett. B* **367**, 60 (1996).
- [23] H. Patberg, *PhD thesis*, Köln, 1995, unpublished.
- [24] M. Allet *et al.*, *Few Body Syst.* **20**, 27 (1996).
- [25] G. Rauprich *et al.*, *Nucl. Phys. A* **535**, 313 (1991).
- [26] J. Zejma, *PhD thesis*, Kraków, 1995, unpublished.
- [27] K. McVoy and L. van Hove, *Phys. Rev.* **125**, 1034 (1962).
- [28] G. Orlandini and M. Traini, *Rep. Prog. Phys.* **54**, 257 (1991).
- [29] J. Golak *et al.*, *Phys. Rev. C* **52**, 1216 (1995).
- [30] R. Schiavilla *et al.*, *Phys. Rev. Lett.* **70**, 3856 (1993).
- [31] D. L. Groep *et al.*, *Phys. Rev. C* **63**, 014005 (2000).
- [32] J. Golak *et al.*, *Phys. Rev. C* **62**, 054005 (2000).
- [33] W. P. Abfalterer *et al.*, *Phys. Rev. Lett.* **81**, 57 (1998).
- [34] J. Golak *et al.*, *Phys. Rev. C* **51**, 1638 (1995).